Int. J. Electrochem. Sci., 13 **(2018)** 5268 – 5283, doi: 10.20964/2018.06.05

International Journal of
ELECTROCHEMICAL
SCIENCE
www.electrochemsci.org

Electrochemical Investigation of Corrosion of Mild Steel in NH_4Cl Solution

Hai-bo Wang[1], *Yun Li*[1], *Guang-xu Cheng*[1,*], *Wei Wu*[1], *Yao-heng Zhang*[2], *Xin-yun Li*[2]

[1] School of Chemical Engineering and Technology, Xi'an Jiaotong University, Xi'an 710049, PR China
[2] Research Institute of Lanzhou Petrochemical Corporation, Lanzhou 730060, PR China
[*]E-mail: gxcheng@mail.xjtu.edu.cn

Received: 9 September 2017 / *Accepted:* 5 March 2018 / *Published:* 10 May 2018

The corrosion from NH_4Cl salt is an important reason for the failure of petroleum refining equipment made of mild steel, especially crude tower overhead system including tower top, overhead piping, and exchanger. The factors affecting the corrosion environment include the surface roughness, dissolved oxygen, temperature, concentration of NH_4Cl, corrosion time, pH, and partial pressure of CO_2. The effects of these environmental factors on the NH_4Cl corrosion of carbon steel were investigated by electrochemical impedance spectroscopy (EIS) and polarization measurements. The EIS results showed that the corrosion process was mainly controlled by the charge transfer process. The polarization measurement results showed that the corrosion rates increased with increasing surface roughness and temperature, but decreased with increasing pH. Decreasing the dissolved O_2 can accelerate the corrosion rate. Cl^- accelerated the dissolution of iron while the NH_4Cl concentration is in the range of 0–1 mol%; and the adsorption of nitrogen in NH_4^+ inhibited the dissolution of iron in 2.5 mol% NH_4Cl solution. The X-ray diffraction surface spectroscopy analysis exhibited that the corrosion products comprise Fe_2O_3, Fe_3O_4, and FeOOH. Besides, the increased CO_2 partial pressure slowed down the corrosion rate of carbon steel in NH_4Cl solution, and the corrosion environment favored the formation of $FeCO_3$ film. This is the first comprehensive study on the effect of corrosion factors on the corrosion rate and will provide guidance for operating conditions in real-time analyses.

Keywords: NH_4Cl; Corrosion factors; Electrochemical; Corrosion behaviors.

1. INTRODUCTION

In recent years, corrosion has been increasing in the crude unit of refining plants in China, presumably because the overhead system of crude unit had more severe operating conditions and complex corrosion environment [1]. The corrosion in the refining plants is commonly caused by the deposited ammonium salts, and has impeded the operational safety of various refining units such as

crude distillation [2], hydroprocessing system [3] and fluidized catalytic cracking unit [4] for many years, resulting in unscheduled equipment replacement and consequently increasing the costs. However, only a few reports discussed the mechanisms of NH_4Cl corrosion, and most of the reports refer to the effect of inhibitor performance [5, 6].

NH_4Cl salts are hygroscopic and very aggressive to carbon steel, alloy steel, and stainless steel [7]. Carbon steel is more cost-effective and is used in the majority (>80%) of refinery components [8]; however, it suffers severe NH_4Cl corrosion, because the deposited NH_4Cl salt will absorb water and create a highly concentrated NH_4Cl corrosive solution [9]. Only a few reports focused on the mechanism of the NH_4Cl corrosion process. There is still a lack of experimental data on NH_4Cl corrosion. Ghosal [10] studied NH_4Cl corrosion in the hydrocracker unit leading to failure and stress corrosion cracking of duplex stainless tubes. Coble [11] reported that excessive use of ammonia as a neutralizer results in significant NH_4Cl fouling. Ou [12, 13] investigated NH_4Cl corrosion and fouling consistently present in the hydrocracking reactor effluent air cooler. Therefore, better understanding of different corrosion environment factors affecting the NH_4Cl corrosion is critical in determining optimal approaches to avoid NH_4Cl corrosion problems.

At present, NH_4Cl corrosion problems are not solved completely, and higher corrosion rate still poses a serious threat to the integrity of refining equipment and the process safety of refineries. Surprisingly, there has been no systematic study on the effect of corrosion environment factors on the corrosion rates in NH_4Cl solution, and thorough understanding of these parameters affecting the corrosion process is still lacking. In this study, the effects of pH, dissolved oxygen, temperature, concentration, exposure time, the partial pressure of CO_2, and surface roughness on the corrosion rate were systematically studied by electrochemical measurement techniques. Based on our very fundamental research of corrosion reactions in realistic NH_4Cl environments, useful corrosion data are provided.

2. EXPERIMENTAL

2.1. Carbon steel specimen

The corrosion specimens were machined from the AISI 20# carbon steel sheet. The nominal elemental composition (wt%) of specimen was 0.21% C, 0.05% Mn, 0.09% P, 0.05% S, 0.38% Si and balance Fe. To create working electrode, an electrical contact to each specimen was provided by a length of copper wire, connected to the back of each specimen mounted in an epoxy resin. The tested surface area of specimens is $1cm^2$.

2.1. Test preparation

All the experiments were conducted in stagnant solutions prepared from analytical grade chemicals and deionized water.

For obtaining different surface roughness, the specimens were unidirectionally ground with different grits of wet sand papers (200, 600, 1000, 1500, and 2000). The surface roughness of the specimens was ground to 600-grit, 1000-grit, 1500-grit and 2000-grit finish using wet sand papers, 2000-grit finish and polished using Al_2O_3 powder (0.001 mm) impregnated polishing cloths. The specimens were cleaned with alcohol and dried in a desiccator until use. The surface roughness experiments were measured by potentiodynamic polarization and EIS in 0.5 mol% NH_4Cl solution for an exposure time of 4 h at 25 ℃.

For obtaining the dissolved oxygen solution, the solutions were saturated by directly bubbling air for 2 h. N_2 was used to deoxygenate the solution during 2 h to obtain the deoxygenated solution. The tests of the effect of dissolved oxygen on the NH_4Cl corrosion of carbon steel were conducted in 0.5 mol% NH_4Cl solution at 25 ℃at an exposure time of 4 h.

The effect of temperature on the NH_4Cl corrosion of carbon steel in 0.5 mol% NH_4Cl solution was investigated by potentiodynamic polarization at five temperatures (25 ℃, 40 ℃, 55 ℃, 70 ℃, and 85 ℃) using a temperature-controlled water bath. The working electrode was exposed to the test solution for 4 h at different temperatures.

A series of experiments were performed in different NH_4Cl concentration solutions (0, 0.1, 0.5, 1.0 and 2.5 mol%) at 55 ℃ for an exposure time up to 4 h.

The effect of exposure time on the NH_4Cl corrosion of carbon steel at five different exposure times (exposures of 1, 2, 4, 8 and 20 h) in 0.5 mol% NH_4Cl solution at 55 ℃ was investigated.

The pH was measured using a pH meter calibrated with standard buffer solutions before each measurement. The pH was adjusted by adding dilute HCl solution, which was prepared by diluting an analytical grade HCl (37%) with deionized water. The specific pH of the solution was 3, 4 and 6, and these solutions were used as the corrosive test environment to simulate the effect of pH on the NH_4Cl corrosion of carbon steel in 0.5 mol% NH_4Cl solution for an exposure time up to 4 h at 55 ℃.

In order to investigate the effect of the partial pressures of CO_2 on the NH_4Cl corrosion of carbon steel, the experiments were conducted in 0.5 mol% NH_4Cl at 55 ℃ at pH 4, and the working electrode was exposed to the test solution for 4 h. The partial pressures of CO_2 (0, 0.4, 0.5, 0.6 and 1.0 atm) in the CO_2/N_2 mixed gas were controlled using two controllers of gas mass flow during the test. The N_2:CO_2 values were 1:0, 3:2, 1:1, 2:3 and 0:1.

2.3. Electrochemical measurements

All the electrochemical tests were performed in a glass cell with a three-electrode system. The reference electrode was a saturated Ag/AgCl electrode; and a platinum wire was used as the counter electrode. The electrochemical experimental procedure was as follows: First, the electrochemical test was carried out when the measured corrosion (open-circuit potential) potential stabilized within ±5 mV over at least 30 min. Then electrochemical impedance spectroscopy (EIS) tests were measured at open circuit potential with a sinusoidal potential excitation of 10 mV amplitude in the frequency range from 100 kHz to 10 mHz. Lastly, the potentiodynamic polarization tests were performed at a sweep rate of 0.5 mV/s.

2.4. X-Ray Diffraction

X-ray diffraction (XRD) measurements were performed using a Rigaku D/max-2400 diffractometer equipped with Cu-Kα radiation as the X-ray source in the 2θ range 5–70°.

3. RESULTS AND DISCUSSION

3.1. Effect of surface roughness on the NH_4Cl corrosion of carbon steel

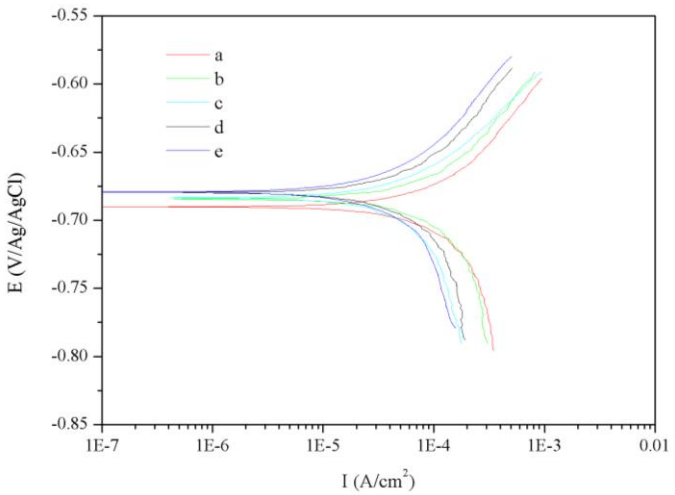

Figure 1. The effect of different surface roughnesses on the polarization curves of carbon steel in a 0.5 mol% NH_4Cl solution for an exposure time of 4 h at 25 °C: (a) surface ground to 600-grit finish; (b) surface ground to 1000-grit finish; (c) surface ground to 1500-grit finish; (d) surface ground to 2000-grit finish; (e) surface ground to 2000-grit finish and polished using Al_2O_3 powder (0.001mm) impregnated polishing cloths.

Table 1. Polarization parameters of polarization curves of the different surface roughnesses in a 0.5 mol% NH_4Cl solution for an exposure time of 4 h at 25 °C.

Surface roughness	B_c (V/decade)	B_a (V/decade)	E_{corr} (V/Ag/AgCl)	$I_{corr} * 10^{-5}$ (A/cm^2)	Corrosion Rate (mm/y)
600-grit finish	–0.148	0.091	–0.688	9.707	1.142
1000-grit finish	–0.123	0.091	–0.687	7.978	0.938
1500-grit finish	–0.136	0.066	–0.683	4.571	0.538
2000-grit finish	–0.124	0.065	–0.674	4.534	0.534
2000-grit finish and polished using Al_2O_3 powder	–0.127	0.088	–0.689	3.927	0.462

Surface roughness depends on various materials depositing directly during the operation process and has a significant effect on the corrosion behavior. Fig. 1 shows the effect of different surface roughnesses on the polarization curves, indicating that both anodic and cathodic reactions are retarded by the presence of smooth surfaces. The relevant electrochemical parameters of the polarization curves at the different surface roughness are listed in Table 1. It is observed that the corrosion rate of smooth surface is lower than that of the roughly polished specimen. The amount of NH_4Cl deposit formed at the metal surface increases with increasing time resulting in a rougher surface and higher corrosion rate.

Further evidence for the effect of different roughnesses of the metal surface is provided by the EIS tests. Fig. 2 shows the EIS plots response at different roughnesses of the metal surface. The relevant equivalent circuit (Fig. 3) was used to fit the EIS data. R_s is the solution resistance, R_p is the resistance of the corrosion products formed on the surface, and R_{ct} is charge transfer resistance. Q_p and Q_{ct} are the constant phase angle elements representing the corrosion product capacitance and double-layer capacitance, respectively. The obtained electrochemical parameters from the electrical equivalent circuit were given in Table 2. The diameter of the capacitive loop decreases with the rougher surface. The polarization resistance value of the smoothest surface estimated from the EIS plots (Fig. 2) is approximately 332 ohm-cm^2, with the least corrosion rate. The corrosion of carbon steel is significantly more severe on the rougher surface, and the rougher surface initiates a much higher pit density [14]. The surface of experimental specimen is polished by using wet sand paper (2000-grit) and Al_2O_3 powder (0.001 mm) impregnated polishing cloths. Therefore, the piping surface should be cleared to remove deposition of various materials in a certain period for effective corrosion protection measurement.

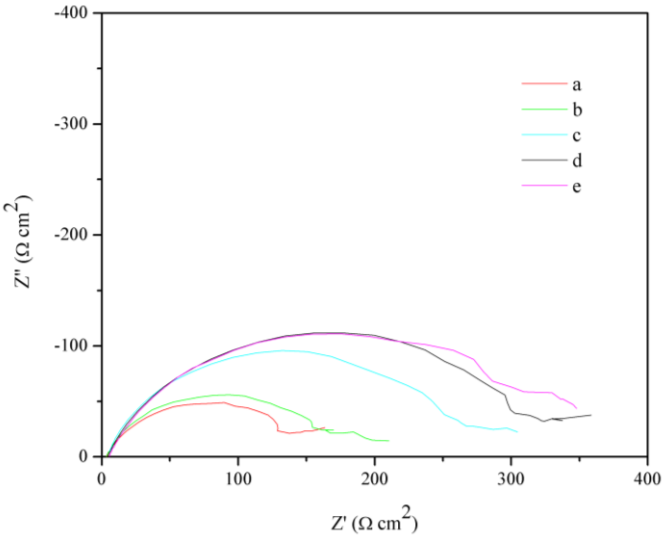

Figure 2. The effect of different surface roughnesses on the EIS of carbon steel in a 0.5 mol% NH_4Cl solution for an exposure time of 4 h at 25 °C: (a) surface ground to 600-grit finish; (b) surface ground to 1000-grit finish; (c) surface ground to 1500-grit finish; (d) surface ground to 2000-grit finish; (e) surface ground to 2000-grit finish and polished using Al_2O_3 powder (0.001mm) impregnated polishing cloths.

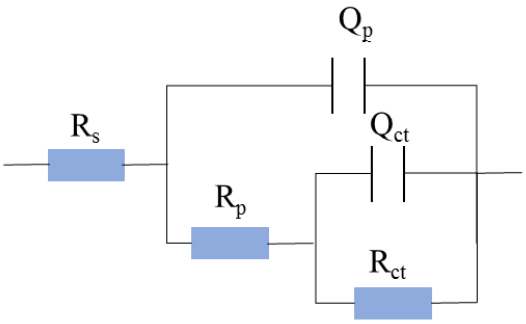

Figure 3. Electrical equivalent circuit used to fit the EIS curves of carbon steel in a 0.5 mol% NH_4Cl solution for an exposure time of 4 h at 25 °C with different surface roughnesses.

Table 2. Electrochemical parameters from the electrical equivalent circuit used to fit the EIS curves of carbon steel in a 0.5 mol% NH_4Cl solution for an exposure time of 4 h at 25 °C with different surface roughnesses.

Surface roughness	R_s	Q_{ct}		R_{ct}	Q_p		R_p
	(Ω cm^2)	(Ω^{-1} cm^{-2} S^n)	n_f	(Ω cm^2)	(Ω^{-1} cm^{-2} S^n)	n_{dl}	(Ω cm^2)
600-grit finish	3.7	9.775×10^{-4}	0.776	140.5	0.128	0.997	36.93
1000-grit finish	3.37	7.951×10^{-4}	0.786	159.4	0.088	0.798	45.29
1500-grit finish	4.382	4.482×10^{-4}	0.823	261.8	0.08	1	19.39
2000-grit finish	4.438	5.024×10^{-4}	0.786	310.2	0.075	0.589	139.9
2000-grit finish and polished using Al_2O_3 powder	5.287	4.535×10^{-4}	0.771	332.2	0.052	1	19.65

3.2. Effect of dissolved oxygen on the NH_4Cl corrosion of carbon steel

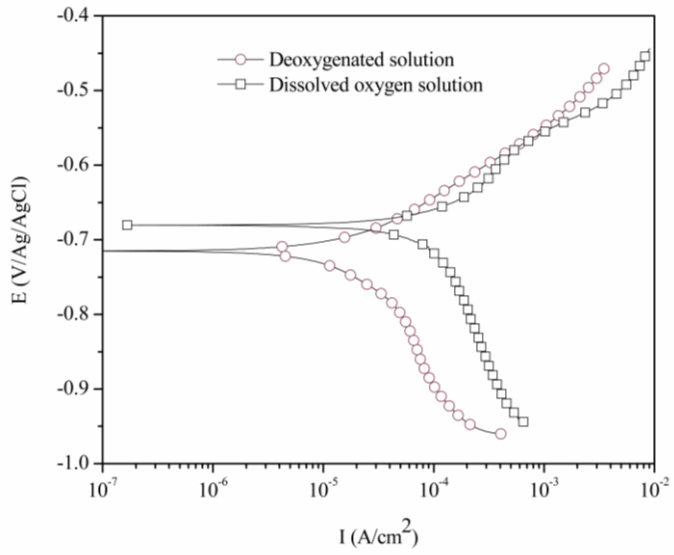

Figure 4. The effect of dissolved oxygen on the polarization curves of mild steel in a 0.5 mol% NH_4Cl solution for an exposure time of 4 h at 25 °C.

Fig. 4 shows that the oxygen reduction process has an important influence on the rate of the cathodic reaction. In the deoxygenized solution, the corrosion rate of mild steel (0.405 mm/y) is slower than that in the dissolved oxygen solution (1.753 mm/y). The reduction of dissolved oxygen accelerates the cathodic reaction, and thus a deoxygenized solution is used for subsequent measurements.

3.3. Effect of temperature on the NH_4Cl corrosion of mild steel

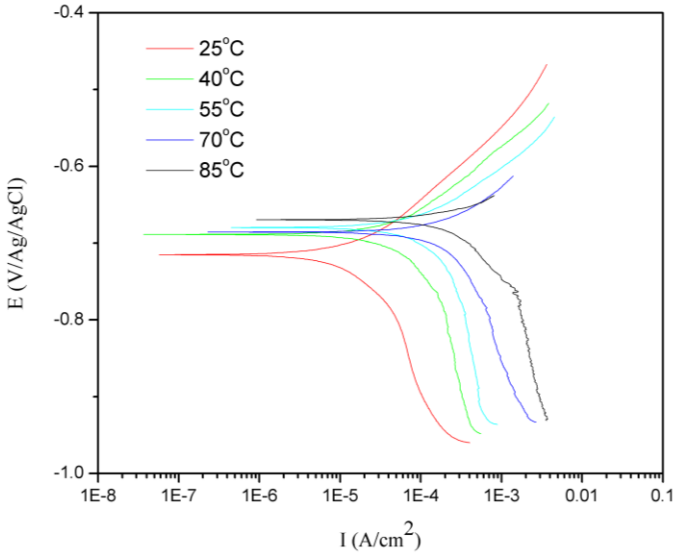

Figure 5. The effect of temperature on the polarization curves of mild steel in 0.5 mol% NH_4Cl solution for an exposure time of 4 h.

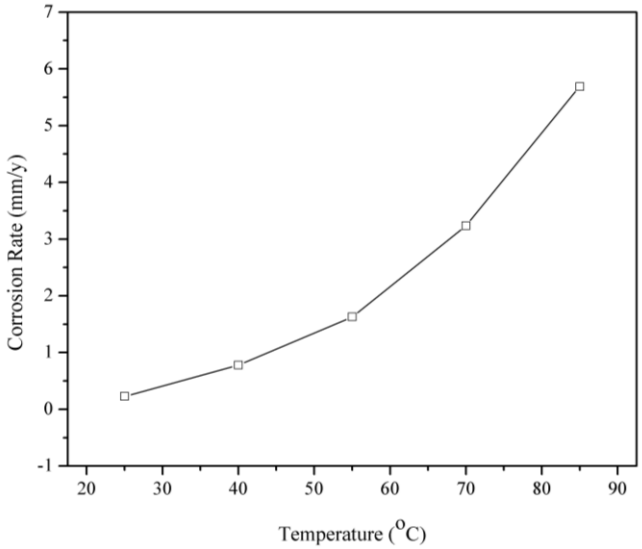

Figure 6. The effect of temperature on the corrosion rates of mild steel in 0.5 mol% NH_4Cl solution for an exposure time of 4 h.

Fig. 5 shows the effect of different temperatures on the NH_4Cl corrosion of mild steel by the polarization curves. The corrosion potential (E_{corr}) and corrosion current density (i_{corr}) increase with increasing temperature in the range 25–85 °C. The corrosion rate is usually directly proportional to temperature. Furthermore, the corrosion rate increases more strongly with increasing temperature at a higher temperature (Fig. 6). For instance, the corrosion rate (5.688 mm/y) reaches to the highest at 85 °C and is consistent with the fact that NH_4Cl corrosion is the most significant at the NH_4Cl deliquescence point. The corrosion rate is under charge-transfer control at room temperature, and becomes mass-transfer limiting current controlled at higher temperatures [15].

3.4. Effect of NH_4Cl concentration on the NH_4Cl corrosion of carbon steel

The changes in the polarization curves at different concentrations of NH_4Cl solutions are shown in Fig. 7. Table 3 shows the polarization parameters obtained from the data in Fig. 7, and the corrosion rates are estimated. The reduction reaction of NH_4^+ is written as Eq. 1. Fe dissolution is given by Eq. 2. The concentration of NH_3 is proportional to the concentration of NH_4Cl (Eq. 1). The limiting current density of the cathodic reaction and the anodic reaction accelerate with increasing concentrations of NH_4Cl solutions from 0 to 1.0 mol%. The corrosion rate increases with increasing concentrations of NH_4Cl solutions from 0 to 1.0 mol%, but at higher NH_4Cl concentrations (2.5 mol%), an opposite trend is observed. The NH_4Cl solution dissociates into NH_4^+ and Cl^-. Cl^- accelerates the dissolution of iron, because chloride can competitively adsorb onto the iron surfaces vs. NH_4^+ between 0 and 1.0 mol% NH_4Cl. The nitrogen of NH_4^+ adsorption inhibits the dissolution of iron and helps maintaining passivity in 2.5 mol% NH_4Cl solution.

$$2NH_4^+ + 2e^- + 2Cl^- \rightarrow 2NH_{3(l)} + H_{2(g)} + 2Cl^- \quad [1]$$

$$Fe - 2e^- \rightarrow Fe^{2+} \quad [2]$$

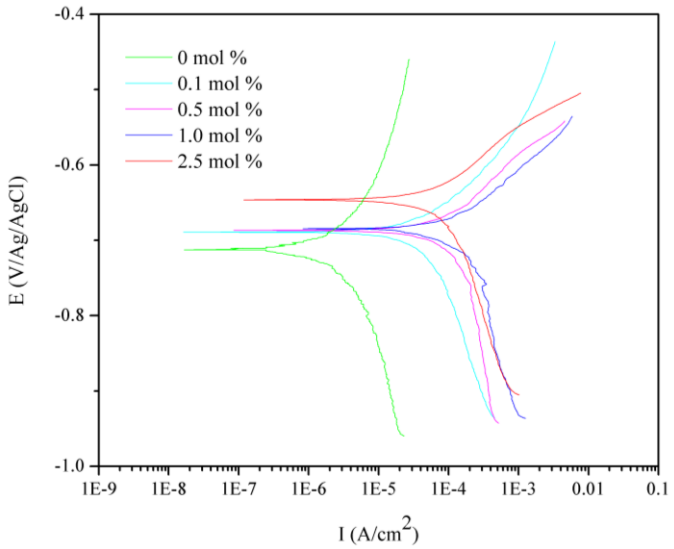

Figure 7. The effect of the different NH_4Cl concentrations on the polarization curves of mild steel for an exposure time of 4 h at 55 °C.

Table 3. Polarization parameters of polarization curves of the different NH_4Cl concentrations for an exposure time of 4 h at 55 °C.

The concentration of NH_4Cl solution (mol%)	B_c (V/decade)	B_a (V/decade)	E_{corr} (V/Ag/AgCl)	$I_{corr} * 10^{-5}$ (A/cm^2)	Corrosion Rate (mm/y)
0	–0.206	0.155	–0.708	0.205	0.024
0.1	–0.274	0.114	–0.689	4.987	0.587
0.5	–0.270	0.082	–0.679	7.691	0.905
1.0	–0.245	0.071	–0.675	10.826	1.273
2.5	–0.248	0.071	–0.634	6.768	0.796

The EIS of the carbon steel at the different NH_4Cl concentrations are shown in Fig. 8. The diameter of the capacitive loop increases with decreasing concentrations of NH_4Cl. The Bode plots exhibit a capacitive loop, corresponding to a charge-transfer resistance (R_{ct}) in parallel with an equivalent capacitance at high frequencies; however, when the NH_4Cl concentration reaches 2.5 mol%, the impedance response of carbon steel has significantly changed. Warburg impedance appears in more concentrated NH_4Cl salt solution, which is the response of diffusion process for NH_4^+ and chloride ions. The EIS data were fitted with the accepted equivalent circuits shown in Fig. 9. There is a solution resistance (R_s) between the reference electrode and the working electrode. R_p is the resistance of the corrosion products formed on the surface, and R_{ct} is charge transfer resistance. Q_p and Q_{ct} are the constant phase angle elements representing the corrosion product capacitance and double-layer capacitance, respectively. W is Warburg impedance in Fig. 9 (b). The impedance parameters obtained following the fitting of the EIS experimental results by using the electrical equivalent circuit displayed in Fig. 9 are listed in Table 4.

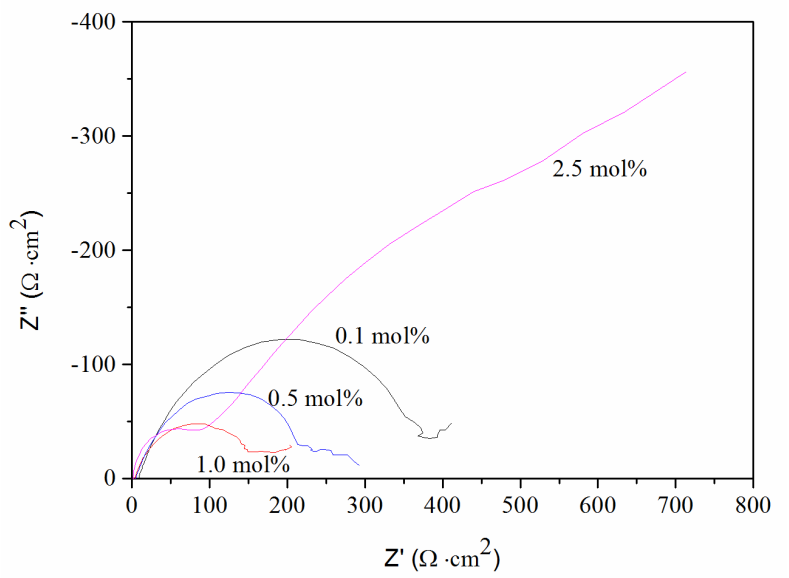

Figure 8. The effect of the different NH_4Cl concentrations on the EIS of mild steel for an exposure time of 4 h at 55 ℃.

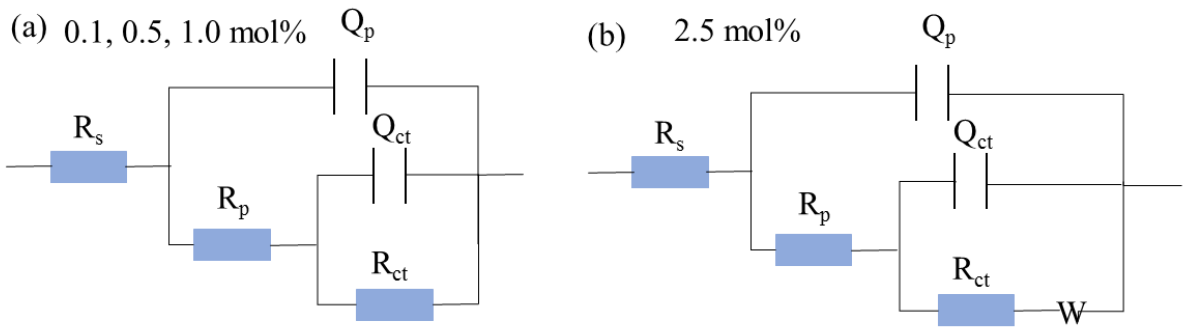

Figure 9. Electrical equivalent circuit used to fit the EIS curves of carbon steel in the different NH_4Cl concentrations for an exposure time of 4 h at 55 ℃.

Table 4. Electrochemical parameters from the electrical equivalent circuit used to fit the EIS curves of carbon steel in the different NH_4Cl concentrations for an exposure time of 4 h at 55 ℃.

NH_4Cl concentration	R_s	Q_{ct}		R_{ct}	Q_p		R_p	W
	(Ω cm^2)	(Ω^{-1} cm^{-2} S^n)	n_f	(Ω cm^2)	(Ω^{-1} cm^{-2} S^n)	n_{dl}	(Ω cm^2)	
0.1 mol%	8.49	5.74×10^{-4}	0.730	382.3	0.289	0.999	68.95	-
0.5 mol%	5.38	4.975×10^{-4}	0.753	254	0.099	0.969	59.64	-
1.0 mol%	4.61	5.33×10^{-4}	0.724	236.9	0.127	1	41.79	-
2.5 mol%	1.54	6.198×10^{-5}	0.996	58.06	2.642×10^{-4}	0.8	30.68	0.0048

3.5. Effect of exposure time on the NH_4Cl corrosion of carbon steel

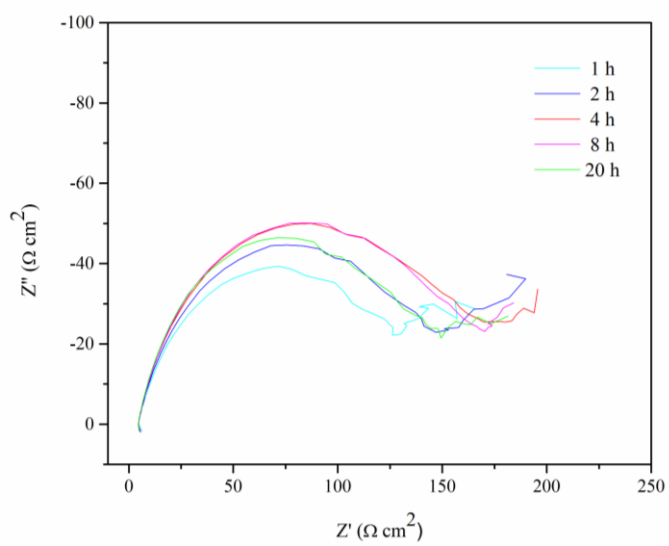

Figure 10. The effect of the exposure time on the EIS of mild steel in 0.5 mol% NH_4Cl solution at 55 ℃.

The EIS results at different exposure times are shown in Fig. 10. The impedance parameters obtained following the fitting of the EIS experimental results by using the relevant equivalent circuit (Fig. 3) were listed in Table 5. The diameter of the capacitive loop reaches a maximum for an exposure

time up to 4 h. Such changes are attributed to the formation of a corrosion product film. The corrosion product film reaches equilibrium and densified for an exposure time up to 4 h, and the corrosion rate reaches minimum.

Table 5. Electrochemical parameters from the electrical equivalent circuit used to fit the EIS curves of carbon steel in 0.5 mol% NH_4Cl solution at 55 ℃ with different exposure time.

Exposure time	R_s	Q_{ct}		R_{ct}	Q_p		R_p
(h)	(Ω cm^2)	(Ω^{-1} cm^{-2} S^n)	n_f	(Ω cm^2)	(Ω^{-1} cm^{-2} S^n)	n_{dl}	(Ω cm^2)
1	5.24	1.363×10^{-3}	0.632	122.9	0.133	0.791	80.44
2	4.96	1.222×10^{-3}	0.639	138.7	0.096	0.725	93.99
4	4.86	1.468×10^{-3}	0.575	180.5	0.535	1	13.03
8	4.96	1.364×10^{-3}	0.602	170.7	0.683	1	12.49
20	4.71	1.509×10^{-3}	0.584	157.6	0.579	0.8	10.89

The structure and composition of the surface corrosion product films formed during corrosion environments of carbon steel are identified by XRD (Fig. 11). Fe_2O_3, Fe_3O_4 and FeOOH characteristic peaks are observed from the XRD spectra of the samples. In NH_4Cl corrosion environment, the first corrosion product formed is iron (II) hydroxide ($Fe(OH)_2$), which forms lepidocrocite (FeOOH) and maghemite (Fe_2O_3). $Fe(OH)_{2(s)}$ is transformed into Fe_3O_4. More background noise is noticeable in these scans, indicating more amorphous phases in the corrosion products.

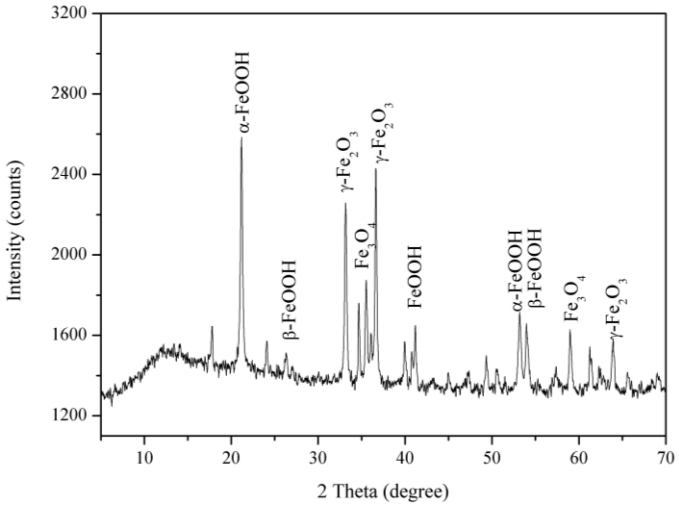

Figure 11. XRD patterns of the corrosion products of carbon steel in 0.5 mol% NH4Cl solution of 4 h at 55 ℃.

3.6. Effect of pH on the NH_4Cl corrosion of carbon steel

Tests are conducted at different bulk solution pH to investigate the effect of pH on the NH_4Cl corrosion of carbon steel. The pH is measured before and after the polarization measurement at each experiment (Table 6). The pH after the test is higher than that before the test. This phenomenon

indicates that a reduction in H^+ proceed as a cathodic reaction. The effect of the pH on the polarization curves is shown in Fig. 12. A clear increase is observed in the cathodic limiting current density with decreasing solution pH, and the anodic branch polarization curves at different pH values are similar. Changing the pH mainly affects the cathodic processes converting the zero current potential into positive intensified the cathodic processes. When the solution pH is increased from 3 to 6, the corrosion potential is diminished. The results (Table 6) reveal that the corrosion current density and the corrosion rate increase with decreasing pH. The EIS results at various pH are shown in Fig. 13. The impedance parameters obtained following the fitting of the EIS experimental results by using the relevant equivalent circuit (Fig. 3) were listed in Table 7. The diameter of the capacitive loop increases with increasing pH. The pH of wet NH_4Cl is <5.0, which is corrosive [16]. Therefore, further experiments are conducted at bulk solution pH maintained at 4 to investigate the possible effect of CO_2 partial pressure.

Table 6. Potentiodynamic polarization parameters of mild steel at different pH in 0.5 mol% NH_4Cl solution for an exposure time up to 4 h at 55 ℃.

Entry	Bulk solution pH		B_c (V/decade)	B_a (V/decade)	E_{corr} (V/Ag/AgCl)	I_{corr} 10^{-5} (A/cm^2)	Corrosion Rate (mm/y)
	Beforce Reaction	After Reaction					
1	3	6.15	–0.167	0.071	–0.674	10.182	1.198
2	4	4.69	–0.172	0.071	–0.685	7.144	0.840
3	6	3.94	–0.198	0.071	–0.693	5.659	0.666

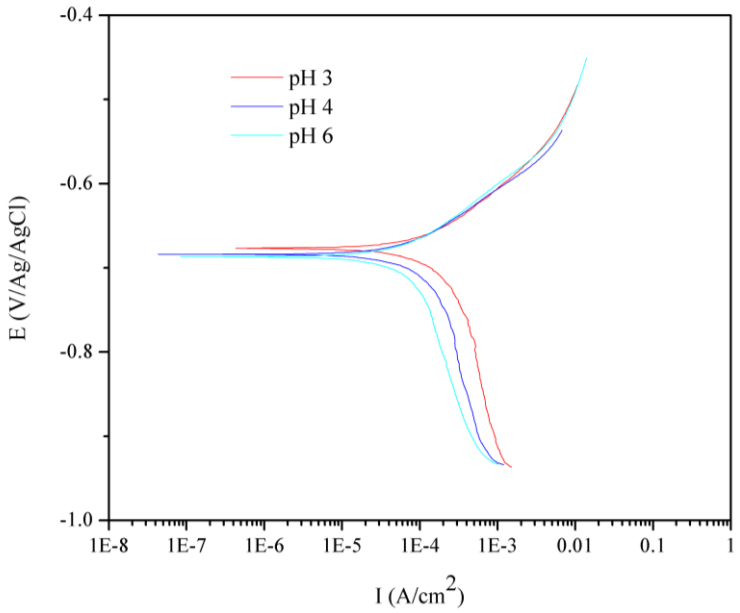

Figure 12. The effect of pH on the polarization curves of carbon steel in 0.5 mol% NH4Cl for an exposure time up to 4 h at 55 ℃.

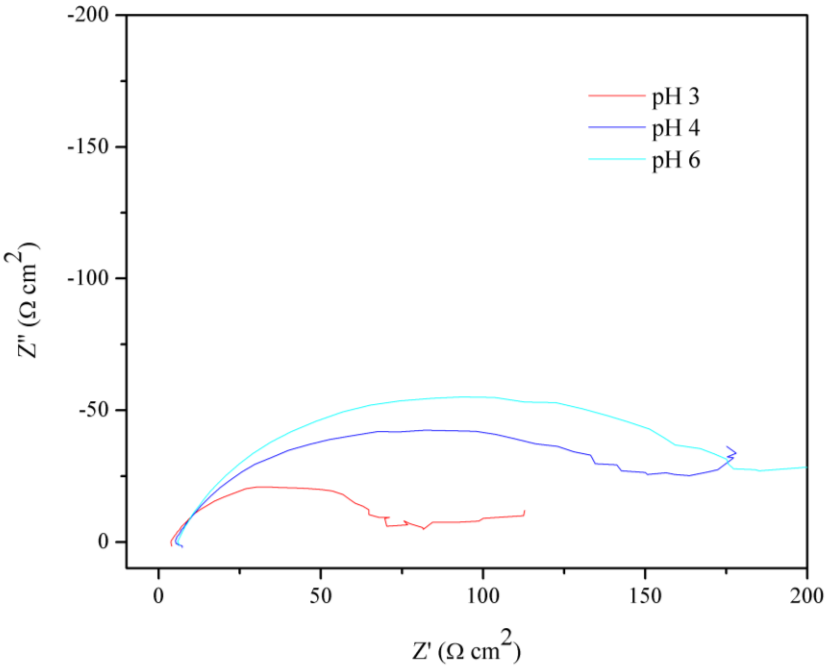

Figure 13. The effect of pH on the EIS of carbon steel in 0.5 mol% NH_4Cl for an exposure time up to 4 h at 55 ℃.

Table 7. Electrochemical parameters from the electrical equivalent circuit used to fit the EIS curves of carbon steel at different pH in 0.5 mol% NH_4Cl solution for an exposure time up to 4 h at 55 ℃.

pH	R_s	Q_{ct}		R_{ct}	Q_p		R_p
	(Ω cm^2)	(Ω^{-1} cm^{-2} S^n)	n_f	(Ω cm^2)	(Ω^{-1} cm^{-2} S^n)	n_{dl}	(Ω cm^2)
3	3.648	1.315×10^{-3}	0.726	69.25	0.123	0.94	13
4	4.704	1.124×10^{-3}	0.708	146.3	0.090	1	29.54
6	5.63	9.534×10^{-4}	0.743	179.3	0.131	1	28.99

3.7. Effect of the partial pressures of CO_2 on the NH_4Cl corrosion of carbon steel

In typical petroleum refinery processing units, such as hydrotreaters, CO_2 may also be present in NH_4Cl salt deposition corrosion. Fig. 14 shows the effect of CO_2 partial pressures on the polarization curves of carbon steel. The relevant electrochemical parameters of the polarization curves at the different partial pressures of CO_2 are listed in Table 8. It is evident from Fig. 14 that the limiting current density of the cathodic reaction and anodic reaction is decreased with increasing CO_2 partial pressure. The corrosion environment favors the film formation favorable, and an increased CO_2 partial pressure may slow down the corrosion rate in the presence of the $FeCO_3$ film. This film slowed down corrosion by presenting a physical diffusion barrier for the species involved in the corrosion process.

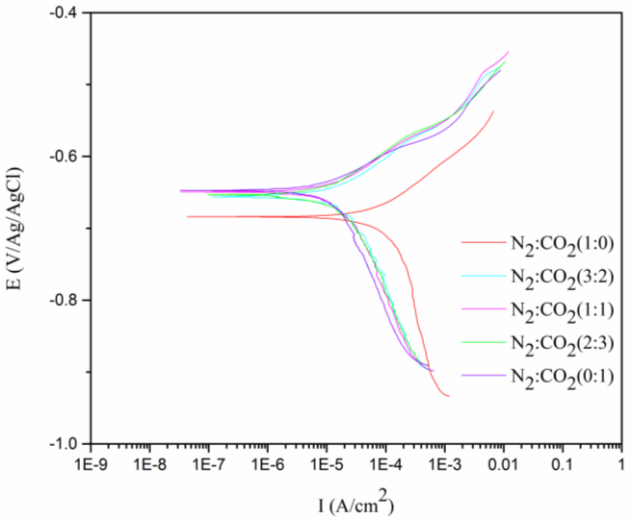

Figure 14. The effect of different partial pressures of CO_2 on the polarization curves of carbon steel in 0.5 mol% NH_4Cl for exposure time up to 4 h at 55 ℃.

Table 8. Polarization parameters of polarization curves of the different partial pressures of CO_2 in 0.5 mol% NH_4Cl for an exposure time of 4 h at 55 ℃.

N_2:CO_2	B_c (V/decade)	B_a (V/decade)	E_{corr} (V/Ag/AgCl)	$I_{corr} * 10^{-5}$ (A/cm^2)	Corrosion Rate (mm/y)
1:0	–0.191	0.083	–0.695	9.927	1.168
3:2	–0.183	0.057	–0.643	1.809	0.213
1:1	–0.180	0.054	–0.642	1.538	0.181
2:3	–0.176	0.054	–0.642	1.529	0.180
0:1	–0.183	0.055	–0.654	1.402	0.165

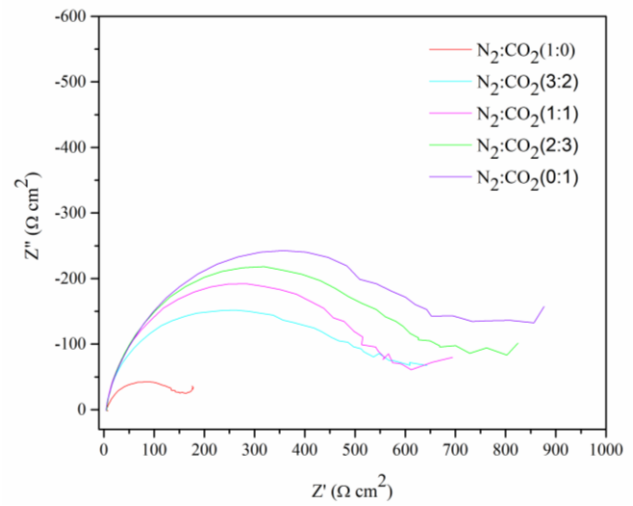

Figure 15. The effect of different partial pressures of CO_2 on the EIS of carbon steel in 0.5 mol% NH_4Cl for exposure time up to 4 h at 55 ℃.

Table 9. Electrochemical parameters from the electrical equivalent circuit used to fit the EIS curves of carbon steel at the different partial pressures of CO_2 in 0.5 mol% NH_4Cl for an exposure time of 4 h at 55 ℃.

N_2:CO_2	R_s	Q_{ct}		R_{ct}	Q_p		R_p
	(Ω cm^2)	(Ω^{-1} cm^{-2} S^n)	n_f	(Ω cm^2)	(Ω^{-1} cm^{-2} S^n)	n_{dl}	(Ω cm^2)
1:0	4.86	1.468×10^{-3}	0.575	180.5	0.535	1	13.03
3:2	4.706	1.798×10^{-4}	0.835	495	0.025	0.8	46.39
1:1	5.1	1.778×10^{-4}	0.857	552.9	0.051	1	35.4
2:3	5.544	1.454×10^{-4}	0.671	559.1	0.006	0.467	42.1
0:1	4.543	2.038×10^{-4}	0.634	730.9	0.016	0.872	225.6

The effect of different partial pressures of CO_2 on the EIS of carbon steel is investigated in 0.5 mol% NH_4Cl for an exposure time up to 4 h at 55 ℃ as shown in Fig. 15. Table 9 showed the impedance parameters obtained following the fitting of the EIS experimental results by using the relevant equivalent circuit (Fig. 3). All the impedance spectra present one single the capacitive loop, indicating that the corrosion behavior is mainly controlled by the charge transfer process. The larger diameter of the capacitive loop corresponds to the better polarization resistance, which has the better protective properties. Noticeably, these capacitive loops are not perfect semicircles, and can be attributed to the frequency dispersion effect as a result of inhomogeneousness of the electrode surface [17]. In the tower overhead system of refining plants, adding a certain amount of CO_2 is considered as an approach to NH_4Cl corrosion problems.

4. CONCLUSIONS

Corrosion behavior of carbon steel in NH_4Cl solution depends on corrosion environment factors such as surface roughness, dissolved oxygen, temperature, the concentration of NH_4Cl, immersion time, pH and the partial pressures of CO_2. The anodic and cathodic reactions are affected by the surface roughness of specimen, and these reactions are retarded by the presence of smooth surfaces. The dissolved oxygen has a significant effect on the rate of the cathodic reaction. The corrosion product reaches equilibrium and densified for an exposure time up to 4 h, and the corrosion rate reaches minimum. The solution pH has a significant effect on the cathodic limiting current density, and the corrosion rate increases with decreasing solution pH. Cl^- accelerates the dissolution of iron between 0 and 1.0 mol% NH_4Cl, and the nitrogen of NH_4^+ adsorption inhibits the dissolution of iron in 2.5 mol% NH_4Cl solution. The corrosion rate increases with increasing temperature more strongly at a higher temperature. The higher partial pressure of CO_2 can result in the formation of stable passive film on the electrode surface, attributing more protective properties.

ACKNOWLEDGMENTS
The authors gratefully acknowledge the financial support of China 973 program (2015CB057602) and the national key research and development program of china (2017YFF0210406).

References

1. K. Toba, M. Ueyama, K. Kawano and J. Sakai, *Corrosion*, 68 (2012) 1049.
2. S. Mahajanam, F. Addington, A. Barba, B. Copple, N. Cuenca, J. Folse and K. Williamson, *NACE International*, New Orleans, Louisiana, 2017, Paper No. 9574.
3. M. Zhu, G.F. Ou, H.Z. Jin, K.X. Wang and Z.J. Zheng, *Eng. Fail. Anal.*, 57 (2015) 483.
4. A. Sun and D. Fan, *NACE International*, San Antonio, Texas, 2010, Paper No. 10359.
5. A.E. Bribri, M. Tabyaoui, B. Tabyaoui, H.E. Attari and F. Bentiss, *Mater. Chem. Phys.*, 141 (2013) 240.
6. P.B. Raja, A.K. Qureshi, A.A. Rahim, H. Osman and K. Awang, *Corros. Sci.*, 69 (2013) 292.
7. K. Toba, K. Kawano and J. Sakai, *NACE International*, San Antonio, Texas, 2014, Paper No. 4007.
8. J. Speight, *Oil and Gas Corrosion Prevention*, (2014) Boston.
9. C.D. Taylor, *Corrosion*, 68 (2012) 591.
10. S. Ghosal, *NACE International*, San Antonio, Texas, 2014, Paper No.3730.
11. N.D. Coble, *NACE International*, Denver, Colorado, 2002, Paper No.02480.
12. G.F. Ou, K.X. Wang, J.L. Zhan, M. Tang, H.H. Liu and H.Z. Jin, *Eng. Fail. Anal.*, 31 (2013) 387.
13. Z.J. Zheng, G.F. Ou, H.J. Ye, H.Z. Jin, L. Sun, K. Huang and J.L. Tan, *Eng. Fail. Anal.*, 68 (2016) 52.
14. Y.J. Chen, R. Howdyshell, S. Howdyshell and L.K. Ju, *Corrosion*, 70 (2014) 767.
15. K.S. George, S. Nešić, *Corrosion*, 63 (2007) 178.
16. H. Lin and V. Lagad, *NACE International*, New Orleans, Louisiana, 2017, Paper No. 8960.
17. M. Lebrini, M. Lagrenée, H. Vezin, M. Traisnel and F. Bentiss, *Corros. Sci.*, 49 (2007) 2254.